Protor-1 is required for efficient mTORC2-mediated activation of SGK1 in the kidney

Laura R Pearce, Eeva M Sommer, Kei Sakamoto, Stephan Wullschleger, Dario R Alessi

Protor-1 is required for efficient mTORC2-mediated activation of SGK1 in the kidney

Laura R. Pearce[1], Eeva M. Sommer[1], Kei Sakamoto[1], Stephan Wullschleger[1], and Dario R. Alessi[1]

1. MRC Protein Phosphorylation Unit, College of Life Sciences, University of Dundee, Dow Street, Dundee DD1 5EH, Scotland.

Correspondence to DRA (d.r.alessi@dundee.ac.uk)

Telephone 44-1382, 344 241 Fax 44-1382, 223 778

Keywords: mTOR, mTORC2, NDRG1, PI3K, Protor/PRR5, SGK1.

Running title: Investigating role of Protor isoforms.

Abstract. The mTOR (mammalian target of rapamycin) protein kinase is an important regulator of cell growth and is a key target for therapeutic intervention in cancer. Two complexes of mTOR have been identified: complex 1 (mTORC1), consisting of mTOR, Raptor and mLST8 and complex 2 (mTORC2) consisting of mTOR, Rictor, Sin1, mLST8 and Protor-1 or Protor-2. Both complexes phosphorylate the hydrophobic motifs of AGC kinase family members: mTORC1 phosphorylates S6K, while mTORC2 regulates phosphorylation of Akt, PKCα and SGK1. To investigate the roles of the Protor isoforms, we generated single as well as double Protor-1 and Protor-2 knockout mice and studied how activation of known mTORC2 substrates was affected. We observed that loss of Protor-1 and/or Protor-2 did not affect the expression of the other mTORC2 components, nor their ability to assemble into an active complex. Moreover, Protor knockout mice display no defects in the phosphorylation of Akt and PKCα at their hydrophobic or turn motifs. Strikingly, we observed that Protor-1 knockout mice displayed markedly reduced hydrophobic motif phosphorylation of SGK1 and its physiological substrate NDRG1 in the kidney. These data suggest that Protor-1 may play a role in enabling mTORC2 to efficiently activate SGK1, at least in the kidney.

Introduction.

mTOR protein kinase plays a key role in controlling cell growth and is likely to be over-activated in the majority of cancers. mTOR exists in two evolutionarily conserved complexes, termed mTOR complex 1 (mTORC1) and mTOR complex 2 (mTORC2) (reviewed in [1]). mTORC1 consists of mTOR bound to Raptor (Regulatory associated protein of mTOR) and mLST8 (mammalian lethal with SEC13 protein 8) and is inhibited by rapamycin [2-4]. mTORC1 is activated downstream of growth factors via the PI3K (phosphoinositide 3-kinase) pathway, involving Akt-mediated phosphorylation of PRAS40 (Proline-rich Akt substrate of 40kDa) and TSC2, leading to activation of the Rheb GTPase [5, 6]. In addition, mTORC1 activity is stimulated by amino acids through a pathway including Rag GTPases and MAP4K3 [7-9]. While mTORC2 also contains mLST8, Raptor is replaced by Rictor (Rapamycin-insensitive companion of mTOR), Sin1 (SAPK-interacting protein 1) and one of the closely related isoforms of Protor-1 or Protor-2 [10-17]. mTORC2 is insensitive to acute rapamycin treatment and although it is also activated by growth factors through an ill-defined PI3K-dependent mechanism.

Some of the best-characterised substrates of mTOR complexes are the Akt, PKC, SGK and S6K protein kinases. These belong to the AGC kinase family and typically members of this family are activated by phosphorylation of two key sites: the T-loop and the hydrophobic motif [18]. mTORC1 controls the hydrophobic motif of p70 ribosomal S6 kinase (S6K) [3, 4], and mTORC2 regulates the equivalent site in Akt [19], protein kinase Cα (PKCα) [11] and serum- and glucocorticoid-induced protein kinase (SGK1) [20], accounting for the ability of mTOR to control protein synthesis, cell proliferation, survival, metabolism and reorganisation of the actin cytoskeleton. Akt (Thr450) and PKCα (Thr638) are also stabilised by phosphorylation of their turn-motif, an event which is mediated by mTORC2 and that probably occurs during translation [21-23]. *SGK1* was originally identified as a serum and glucocorticoid-inducible gene and it is activated downstream of insulin and growth factors (reviewed in [24]). The generation of PtdIns(3,4,5)P_3 by PI3-kinase triggers a signalling cascade that leads to the phosphorylation of the hydrophobic motif (Ser422 in SGK1) by mTORC2 [20]. This does not directly activate SGK1, but instead creates a docking site for PDK1, which can subsequently phosphorylate SGK1 at the T-loop residue (Thr256), resulting in its activation [25, 26]. One of the best-characterised substrates of SGK1 is NDRG1 and the phosphorylation of this protein is frequently used as a marker for SGK1 activity [20, 27].

Protor-1 and Protor-2 isoforms are encoded by different genes and interact with Rictor through a conserved N-terminal region [15-17]. This may stabilise Protor, as total protein levels of Protor are vastly reduced in Rictor knockout fibroblasts [15]. As Protor isoforms have no other obvious functional domains it is hard to predict their physiological function. To address how Protor isoforms influence mTORC2 we generated single Protor-$1^{-/-}$, Protor-$2^{-/-}$ as well as Protor-$1^{-/-}$Protor-$2^{-/-}$ double knockout mice. While phosphorylation of the hydrophobic and turn motifs of both Akt and PKCα was unaffected in Protor-$1^{-/-}$ mice, we observed a significant reduction in phosphorylation of the hydrophobic motif of SGK1 in kidney, a tissue in which SGK1 phosphorylation and activity is high. Protor-1 deficient mice also displayed a marked reduction in phosphorylation of the SGK1 T-loop and also that of NDRG1, a specific SGK1 substrate. Our results indicate that Protor-1 plays a critical role in mediating the phosphorylation of SGK1 by mTORC2 in the kidney.

Materials and methods.

Materials. Glutathione Sepharose, Protein G-Sepharose and Protein A-agarose were purchased from Amersham Bioscience. IGF1 was from Cell Signaling Technology. Tween-20, DMSO and dimethyl pimelimidate were from Sigma and CHAPS was from Calbiochem.

Antibodies. The following antibodies were raised in sheep and affinity purified on the appropriate antigen: anti-NDRG1 (S276B, 3rd bleed; raised against the full length human protein, used for immunoblotting), anti-phospho-NDRG1 which recognises NDRG1 phosphorylated at Thr346, Thr356 and Thr366 (S911B, 2nd bleed; raised against [CRSRSHTpSEG], used for immunoblotting), anti-Akt1 (S742B, 3rd bleed; raised against the full length human protein, used for immunoblotting), anti-PRAS40 (S115B, 1st bleed; residues 238 - 256 of human PRAS40 [DLPRPRLNTSDFQKLKRKY], used for immunoblotting), anti-phospho-PRAS40 which recognises PRAS40 phosphorylated at Thr246 (S114B, 2nd bleed; raised against residues 240 - 251 of human PRAS40 [CRPRLNTpSDFQK], used for immunoblotting), anti-Protor-1 (S020C, 3rd bleed; raised against the full length human protein, used for immunoprecipitation and immunoblotting), anti-Protor-2 (S136C, 3rd bleed; raised against the full length human protein, used for immunoprecipitation and immunoblotting), anti-Rictor (S274C, 1st bleed; raised against residues 6-20 of mouse Rictor [RGRSLKNLRIRGRND], used for immunoblotting), anti-Sin1 (S008C, 2nd bleed; raised against full length human Sin1, used for immunoprecipitation and immunoblotting) and anti-SGK1 (S515A, 2nd bleed; raised against full length human SGK1, used for immunoprecipitation and immunoblotting). The total SGK1 (#5188) and the gamma-ENaC antibodies were purchased from Sigma. The antibody recognizing the alpha-subunit of ENaC was a kind gift of S. Wilson (Dundee University) and R.C. Boucher (University of North Carolina at Chapel Hill). The total mTOR (#sc-1549), phospho-SGK1 Ser422 (#sc16745) and flotillin-1 (#sc-25506) antibodies were purchased from SantaCruz Biotechnology. The phospho-Akt Ser473 (#9271), Thr308 (#4056), phospho-IGF1/Insulin receptor (#3024), IGF1 receptor (#3027), total FoxO1 (#2880), phospho-FoxO1/3 (#9464) and GAPDH (#2118) antibodies were purchased from Cell Signaling Technology. For immunoblotting of the phosphorylated T-loop of SGK1 we employed the pan-PDK1 site antibody from Cell Signaling Technology (#9379).

General methods. Tissue culture, immunoblotting, restriction enzyme digests, DNA ligations, and other recombinant DNA procedures were performed using standard protocols. DNA constructs used for transfection were purified from *E. coli* DH5α using a Qiagen plasmid Mega or Maxi kit according to the manufacturer's protocol. All DNA constructs were verified by DNA sequencing, which was performed by DNA sequencing & services (MRCPPU, College of Life Sciences, University of Dundee, Scotland, www.dnaseq.co.uk) using Applied Biosystems Big-Dye Ver 3.1 chemistry on an Applied Biosystems model 3730 automated capillary DNA sequencer.

Generation, genotyping and maintenance of Protor-1$^{-/-}$, Protor-2$^{-/-}$ and Protor-1$^{-/-}$ Protor-2$^{-/-}$ mice. Protor-1$^{fl/+}$ and Protor-2$^{fl/+}$ mice were generated by TaconicArtemis as described in Figure 1. Protor-1$^{+/fl}$ mice were crossed with Bal1Cre$^{+/-}$ mice which express Cre recombinase in all tissues [28], enabling the generation of mice containing one Protor-1 knockout allele (Protor-1$^{+/-}$). These heterozygous mice were then crossed together in order to obtain whole-body Protor-1 knockout mice (Protor-1$^{-/-}$). Whole-body Protor-2$^{-/-}$ mice were generated using the same strategy. The mice were maintained on a C57BL/6J background and genotyping was carried out by PCR using genomic DNA isolated from ear or tail biopsies. For Protor-1 mice, Primer 1 (5'-GAGTTCATCTTCAAACCCAAGC-3'), Primer 2 (5'-CCCGTGCCAGATTAACATGG-3') and Primer 6 (5'-

TCAACATGACGAAGTCAAGTGTC-3') were used to detect the wild type, heterozygous and knockout alleles. For Protor-2 mice, Primer 1 (5'-AACCTGGGAAAGGAAGAAGC-3'), Primer 2 (5'-GCACTCAAAATCTCTGTGGC-3') and Primer 4 (5'-TCTGATTCTCCCACCTGAAGT-3') were utilized. The PCR programme consisted of 5min at 95°C, 35 cycles of 30sec at 95°C, 30sec at 60°C and 1min at 72°C, followed by 10min at 72°C on a PTC-200 Peltier Therma Cycler DNA engine. Mice were maintained under specific pathogen-free conditions and routine animal ear notching for genotyping was carried out by staff in the College of Life Science Transgenic Unit (University of Dundee). All procedures were carried out in accordance with the regulations set by the University of Dundee and the United Kingdom Home Office.

Blood glucose and plasma insulin measurement. Blood glucose levels were measured using the Ascensia Breeze 2 blood glucose monitoring system (Bayer) following tail incision. For plasma insulin measurements, blood was collected in haematocrit capillary tubes (Hawksley) from mice following tail incision and incubated on ice. Blood was centrifuged at 3,000xg for 15min to obtain plasma. Insulin levels were measured using a rat/mouse insulin enzyme-linked immunosorbent assay (ELISA) kit (Millipore, EZRMI-13K). Assays were carried out according to the manufacturer's instructions, typically this involved the use of 5µl of plasma per assay and mouse insulin standards from 0 to 10ng/ml were used to generate a standard curve. Samples were assayed in duplicate.

Glucose tolerance test. Mice were deprived of food overnight (16hrs), weighed and basal blood glucose levels measured following tail incision. Mice were injected intraperitoneally with 2mg/g D-glucose solution and blood glucose levels measured at 15, 30, 45, 60 and 120min post-injection.

Insulin tolerance test. Mice were allowed to feed overnight ad libitum and then food was removed for 3hrs before the experiment. Mice were weighed and the basal blood glucose level determined following tail incision. Mice were then injected intraperitoneally with 1mU/g insulin and blood glucose levels measured at 15, 30, 45, 60 and 120min post-injection.

Injection of mice with IGF1. Mice were starved for 3hrs before being anaesthetised using sodium pentobarbital (80-90µg/g, intraperitoneally injected) and placed on a heating pad to maintain body temperature. This was followed by an intravenous injection through the inferior vena cava of either PBS or 0.5µg/g IGF1 dissolved in PBS [29]. Tissues were rapidly excised 5min after injection and frozen in liquid nitrogen.

Buffers. The following buffers were used: Tris-CHAPS lysis buffer [50mM Tris-HCl (pH 7.5), 1mM EGTA, 1mM EDTA, 0.3% (w/v) CHAPS, 1mM sodium orthovanadate, 10mM sodium-ß-glycerophosphate, 50mM sodium fluoride, 5mM sodium pyrophosphate, 0.27M sucrose, 0.15M NaCl, 0.1 % (v/v) 2-mercaptoethanol, 1mM benzamidine and 0.1mM phenylmethylsulphonylfluoride], Buffer A [50mM Tris-HCl (pH 7.5), 0.1mM EGTA and 0.1% (v/v) 2-mercaptoethanol], Hepes-CHAPS lysis buffer [40mM Hepes (pH 7.5), 120mM NaCl, 1mM EDTA, 0.3% (w/v) CHAPS, 10mM sodium pyrophosphate, 10mM sodium-ß-glycerophosphate, 50mM sodium fluoride, 0.5mM sodium orthovanadate, 1mM benzamidine and 0.1mM phenylmethylsulphonylfluoride], Hepes kinase buffer [25mM Hepes (pH 7.5), 50mM KCl], TBS-Tween Buffer [50mM Tris-HCl pH 7.5, 0.15M NaCl and 0.1% (v/v) Tween-20] and Sample Buffer [50mM Tris-HCl pH 6.8, 6.5% (v/v) Glycerol, 1% (w/v) SDS, and 1% (v/v) 2-mercaptoethanol].

Preparation of tissue lysates. Mouse tissues were rapidly excised, snap frozen in liquid nitrogen and stored at -80°C until use. Frozen tissues were weighed and homogenised in a 10-fold excess of ice-cold Tris-CHAPS or Hepes-CHAPS lysis buffer using a polytron. Lysates were centrifuged at 3,000rpm for 15min at 4°C and supernatants then further centrifuged at 12,000rpm for 20min at 4°C to remove all insoluble material. The protein concentration of each lysate was determined before being snap frozen in aliquots and stored at -80°C.

Purification of inactive GST-Akt1 and GST-ΔN-SGK1 [61-431] from HEK293 cells 10cm diameter dishes of HEK293 cells were cultured and each dish was transfected with 5μg of either GST-Akt1 or GST-ΔN-SGK1 [61-431] using the polyethylenimine (PEI) method. 24hrs post-transfection, HEK293 cells that had been transfected with GST-Akt1 or GST-ΔN-SGK1 [61-431] were serum starved for 16hrs. Cells were treated with 1μM PI-103 for 30min and harvested in Tris-CHAPS lysis buffer. 3mg Lysate was affinity purified on 10μl glutathione-Sepharose for 1hr at 4°C on a rotating wheel. The resulting precipitates were washed twice with Tris-CHAPS lysis buffer, twice with Buffer A and twice with Buffer A containing 0.27M sucrose. GST-tagged proteins were eluted from the resin by resuspension in an equal amount of Buffer A containing 0.27M sucrose and 10mM glutathione (pH7.5-8) for 1hr on ice. Supernatants were filtered through a 0.22μm-spin column and aliquots were snap-frozen and stored at -80°C.

mTORC2 activity assays. Mouse tissues or MEFs were lysed in Hepes-CHAPS lysis buffer and 1-4mg of lysate was pre-cleared by incubation with 5μl of Protein G-Sepharose conjugated to pre-immune IgG. The lysates were then incubated with 5μl of Protein G-Sepharose covalently conjugated to either 5μg anti-Sin1 antibody, or 5μg pre-immune IgG for 2hrs at 4ºC on a vibrating platform. The immunoprecipitates were washed four times with Hepes-CHAPS lysis buffer, followed by two washes with Hepes kinase buffer. Assays were carried out in a final volume of 40μl Hepes kinase buffer containing 1μg GST-Akt1 or 1μg GST-ΔN-SGK1 [61-431] and kinase reactions initiated upon addition of 0.1mM ATP and 10mM $MgCl_2$. Reactions were carried out for 30min at 30ºC on a vibrating platform and stopped by the addition of SDS sample buffer. Samples were heated to 70ºC for 5min, passed through a Spin-X column and subjected to electrophoresis and immunoblot analysis.

Immunoprecipitation of endogenous Protor-1, Protor-2. 1mg (for Protor-1 immunoprecipitates) or 2mg (for Protor-2 immunoprecipitates) lysate from each of the indicated tissues was pre-cleared by incubation with 5μl of Protein G-Sepharose for 30min. The lysates were then incubated with 5μg of anti-Protor-1 or anti-Protor-2 covalently coupled to Protein G-Sepharose for 1.5hrs at 4°C. Immunoprecipitates were washed four times with Tris-CHAPS lysis buffer lacking 2-mercaptoethanol and twice with Buffer A in which reducing agent was omitted. Immunoprecipitates were resuspended in 20μl of SDS sample buffer (lacking reducing agent) and filtered through a Spin-X column to remove the Sepharose resin. 1X NuPAGE reducing agent (Invitrogen) was added to the eluted samples. These were then subjected to electrophoresis and immunoblot analysis as described below.

Kidney membrane preparations for ENaC immunoblots. This was undertaken as previously described [30]. Harvested mouse kidneys were snap frozen immediately after isolation and homogenized in detergent-free lysis buffer containing 50mM Tris pH 7.5, 1mM EDTA, 1mM EGTA, 1mM sodium orthovanadate, 5 mM sodium fluoride, 5 mM sodium pyrophosphate, 0.27M sucrose, 0.1% (v/v) 2-mercaptoethanol and protease inhibitors (1 tablet per 50ml) with a Polytron homogenizer. Nuclei and debris were pelleted by centrifugation at 1,500 g for 5min. The procedure was repeated at 3,000 g for 10min and the low speed supernatants were next centrifuged at 100,000 g for 1 hour. The

pellet was washed with 1 volume of lysis buffer without reducing agent and centrifuged again at 100,000g for 15 min to remove any remaining cytosolic particles. The pellet was then resuspended in lysis buffer including 1% (v/v) NP40 and centrifuged at 16,500g for 10min. The protein content of the membrane preparations was quantified and resuspended in SDS sample buffer.

Immunoblotting. Tissue or cell lysates (10-20µg) or immunoprecipitated samples were heated at 70°C for 5min in sample buffer, and subjected to polyacrylamide gel electrophoresis and electrotransfer to nitrocellulose membranes. Membranes were blocked for 1hr in TBS-Tween buffer containing 5% (w/v) skimmed milk. The membranes were probed with the indicated antibodies in TBS-Tween containing 5% (w/v) skimmed milk or 5% (w/v) BSA for 16hrs at 4°C. Detection was performed using horseradish peroxidase-conjugated secondary antibodies and enhanced chemiluminescence reagent.

Generation and stimulation of MEFs (mouse embryonic fibroblasts)
MEFs isolated from mouse embryos at E13.5 (embryonic day 13.5) were generated and cultured as described previously [31]. Cells were serum-starved in DMEM for 16h prior to stimulation with 50ng/ml IGF1 for 30min. Cells were subsequently lysed and the lysates centrifuged at 18000g for 15min at 4°C. Supernatants were snap-frozen and stored at −80 °C. Lysates (10µg) were analysed by immunoblotting using the antibodies indicated in the figures.

Results.

Generation of Protor-1$^{-/-}$, Protor-2$^{-/-}$ and Protor-1$^{-/-}$Protor-2$^{-/-}$ knockout mice. To study the physiological role of the Protor isoforms, we generated Protor-1$^{-/-}$ and Protor-2$^{-/-}$ knockout mice as described in the materials and methods and Figure 1. The breeding strategy for the single Protor-1$^{-/-}$ and Protor-2$^{-/-}$, as well as the Protor-1$^{-/-}$Protor-2$^{-/-}$ double knockout mice is summarised in Table 1. Mice were generated and maintained on a pure C57BL/6J background. The single and double knockout mice were viable, born at the expected Mendelian frequency (Table 1) and did not display any overt phenotype. The genotype of the Protor-1$^{-/-}$ and Protor-2$^{-/-}$ mice was verified by PCR (Figure 1C&G). In order to confirm the ablation of protein expression, Protor-1 was immunoprecipitated from the tissues of the Protor-1$^{-/-}$ mice and as expected, there was a reduction in Protor-1 expression of approximately 50% in the Protor-1$^{+/-}$ mice and Protor-1 could not be detected in the homozygous knockout mice (Figure 1D). A similar result was also obtained in the Protor-2$^{-/-}$ mice (Figure 1H). There was no significant difference in the body weight of male or female single Protor-1$^{-/-}$ or Protor-2$^{-/-}$ or Protor-1$^{-/-}$Protor-2$^{-/-}$ double knockout mice compared to wild type mice up to 4 months of age (data not shown). In addition, the Protor-1$^{-/-}$ knockout animals displayed normal blood glucose and plasma insulin levels under both fasted and fed conditions and there was no detectable change in whole body glucose or insulin tolerance compared to wild type animals (Supplementary Figure 1).

NDRG1 phosphorylation is diminished in the kidney of Protor-1$^{-/-}$ knockout mice. We initially examined the phosphorylation state of Akt, its substrate PRAS40 and FoxO1 as well as NDRG1, an SGK1 substrate, in various tissues from fed littermate Protor-1$^{+/+}$, Protor-1$^{+/-}$ and Protor-1$^{-/-}$ mice. This revealed no significant difference in Akt, PRAS40 or FoxO1 phosphorylation in any of the tissues examined among the three genotypes (Figure 2). The only tissue in which significant phosphorylation of NDRG1 was observed in the kidney of Protor-1$^{+/+}$ animals (Figure 2A). Consistent with this the NDRG1 protein migrated as several electrophoretic species in kidney and only as a single species in other tissues. Interestingly, there was a partial reduction in the phosphorylation of NDRG1 in the kidney of Protor-1$^{+/-}$ animals and this was more pronounced in the Protor-1$^{-/-}$ knockouts (Figure 2A).

We next investigated NDRG1 phosphorylation in kidney extracts derived from single and double Protor-1 and Protor-2 knockout animals. Although there was no change in NDRG1 phosphorylation in the kidney of single Protor-2$^{-/-}$ mice (Figure 3B), the Protor-1$^{-/-}$Protor-2$^{-/-}$ double knockout mice displayed reduced NDRG1 phosphorylation, similar to that seen in the single Protor-1$^{-/-}$ knockouts (Figure 3C). In all cases Akt (Thr308 and Ser473) and PRAS40 phosphorylation was unaffected by the loss of Protor-1 and/or Protor-2. In addition, the phosphorylation of Akt and PKCα at the turn motif (Thr450 and Thr638 respectively) and the PKCα hydrophobic motif (Ser657) remained unchanged in the kidney of the Protor isoform knockout mice (Figure 3A-C). We also investigated phosphorylation of mTORC2 targets in the lung and liver tissues of the single Protor-2$^{-/-}$ mice as well as the Protor-1$^{-/-}$Protor-2$^{-/-}$ double knockout mice. This confirmed that there was no substantial phosphorylation of NDRG1 detected in these tissues and that phosphorylation of Akt and its substrates PRAS40 and FoxO1 was not reduced in the Protor-deficient animals (Supplementary Figure 2).

IGF1-induced SGK1 phosphorylation is reduced in the kidney of Protor-1$^{-/-}$ knockout mice. To investigate further the role that Protor-1 plays in regulating SGK1 activation in the kidney, single and double Protor-deficient mice were injected intravenously with 0.5μg/g IGF1 for 5min to activate the PI3K pathway in a wide variety of tissues (instead of limited insulin-sensitive tissues). Tissue extracts derived from these animals were probed using antibodies that recognise SGK1 phosphorylated at its

hydrophobic motif (Ser422) as well as its T-loop residue (Thr256). While SGK1 hydrophobic motif phosphorylation was stimulated upon IGF1 treatment in the wild type control mice, phosphorylation of this site was barely detectable in the single Protor-1$^{-/-}$ mice (Figure 4A) or Protor-1$^{-/-}$Protor-2$^{-/-}$ double knockout mice (Figure 4C). Consistent with phosphorylation of Ser422 being required for the subsequent phosphorylation of Thr256 [25], there was also no phosphorylation of Thr256 in these animals. The loss of Ser422 and Thr256 phosphorylation would result in a lack of SGK1 activation, which accounts for the much-reduced phosphorylation of NDRG1. In contrast, SGK1 and NDRG1 were phosphorylated to the same extent in kidney extracts derived from wild type and single Protor-2$^{-/-}$ knockout mice (Figure 4B). There was also no significant difference in the IGF1-induced phosphorylation of Akt at either Ser473 or Thr308 or that of PRAS40 in the kidney of Protor-1 and/or Protor-2 deficient mice (Fig 4).

NDRG1 phosphorylation was also assessed in response to IGF1 stimulation in the liver of the single and Protor-1$^{-/-}$Protor-2$^{-/-}$ double knockout mice (Supplementary Fig 3). We observed that IGF1 did not lead to a marked increase in NDRG1 phosphorylation and consistent with this did not induce an electrophoretic band-shift of the total NDRG1 protein under conditions in which Akt and its substrate PRAS40 were phosphorylated (Supplementary Fig 3). We also generated mouse embryonic fibroblasts (MEFs) derived from wild type and Protor-1$^{-/-}$Protor-2$^{-/-}$ double knockout mice and found that IGF1 induced a significant phosphorylation and an electrophoretic band-shift of NDRG1 protein in both wild type and Protor-1$^{-/-}$Protor-2$^{-/-}$ double knockout MEFs (Fig 5). This observation is considered further in the Discussion.

mTORC2 formation is unaffected by the loss of Protor-1 and Protor-2. Previously it was reported that loss of the mTORC2 component Sin1 affects the ability of mTOR and Rictor to interact [12-14]. As reduced mTORC2 complex formation could potentially account for the decreased phosphorylation of SGK1, the ability of mTOR, Rictor and Sin1 to bind one another was investigated in the Protor-1$^{-/-}$ and Protor-2$^{-/-}$ single and double knockout animals. mTOR and Rictor still co-immunoprecipitated with Sin1, irrespective of the presence of either Protor-1 or Protor-2 in kidney (Figure 6A-C). This provides evidence that Protor-1 and Protor-2 are not essential for mTORC2 complex assembly.

Protor isoforms are not required for mTORC2 kinase activity *in vitro*. We next investigated whether Protor isoforms are required for the kinase activity of mTORC2. mTORC2 was immunoprecipitated using the Sin1 antibody from either fed (Fig 7A & B) or IGF1-injected (Fig 7C & D) wild type or double Protor-1$^{-/-}$ and Protor-2$^{-/-}$ knockout mouse kidney or liver lysates and its ability to phosphorylate GST-Akt1 or GST-SGK1 assessed. These studies revealed that loss of Protor isoforms did not significantly impact on the ability of immunoprecipitated mTORC2 to phosphorylate GST-Akt1 or GST-SGK1 in cell free-assays. Similar results were obtained when mTORC2 activity was assayed in the Protor-1$^{-/-}$Protor-2$^{-/-}$ double knockout MEFs (Fig 7E & F). These findings indicate that Protor isoforms are dispensable for regulating intrinsic mTORC2 kinase activity.

Discussion.

The results presented in this study indicate that in contrast to the other mTORC2 specific components Sin1 and Rictor, Protor subunits are not essential for mouse viability, growth, mTORC2 complex assembly or phosphorylation of the hydrophobic and turn motifs of Akt. Studies using tissue-specific knockouts of Rictor in both muscle and adipose have demonstrated the key role mTORC2 plays in insulin signalling and glucose homeostasis. Muscle-specific Rictor$^{-/-}$ mice have defective insulin-stimulated glucose uptake in muscle and are glucose intolerant [32], while adipose-specific knockouts of Rictor display impaired glucose uptake and reduced whole body insulin sensitivity [33, 34]. However we did not observe any significant defects in glucose clearance and insulin sensitivity, consistent with Akt Ser473 phosphorylation being unaffected in the single or Protor-1$^{-/-}$Protor-2$^{-/-}$ double knockout mice. These observations indicate that the role of Protor-1 is distinct from that of Rictor and is not required for activation of Akt, at least under the conditions that we have studied.

Instead, our data suggest that Protor-1 is required for efficient activation of SGK1 in the kidney, the only tissue in which we were able to measure significant endogenous hydrophobic and T-loop motif phosphorylation of SGK1 and that of its substrate NDRG1. Interestingly, Protor-1 expression was previously shown to be high in the kidney, perhaps indicating the key role Protor-1 plays in this tissue [15]. Our data also indicate that Protor-1 rather than Protor-2 is critical for efficient activation of SGK1 in the kidney, as defects in SGK1 and NDRG1 phosphorylation were not observed in the Protor-2 knockout animals. Moreover, the Protor-1$^{-/-}$Protor-2$^{-/-}$ double knockout mice displayed identical reductions in SGK1 and NDRG1 phosphorylation to the single Protor-1$^{-/-}$ deficient mice, emphasising that Protor-1 rather that Protor-2 is key for regulating SGK1 activation in the kidney.

In contrast to what was observed in kidney tissues, IGF1 induced a significant phosphorylation and an electrophoretic band-shift of NDRG1 protein in both wild type and Protor-1$^{-/-}$Protor-2$^{-/-}$ double knockout MEFs, suggesting that the effects of Protor on SGK1 activation and NDRG1 phosphorylation may be specific to the kidney. In our hands, endogenous SGK1 protein in MEFs is undetectable using antibodies that readily detect SGK1 in the kidney. It is possible that when SGK1 levels are low, much higher levels of Akt or a distinct kinase contribute to observed NDGR1 phosphorylation in MEFs. Moreover, SGK2 or SGK3 which we did not assess, may not be regulated by Protor isoforms and if this was the case might account for observed NDGR1 phosphorylation in Protor deficient MEFs.

The best-characterised role of SGK1 *in vivo* is in the kidney where it stimulates sodium transport into epithelial cells by enhancing the stability and expression of the epithelial sodium channel (ENaC) (reviewed in [35]). The expression of ENaC is typically maintained at a low level by ubiquitination and degradation. SGK1 phosphorylates the HECT E3 ubiquitin ligase, Nedd4.2, preventing its interaction with ENaC and hence preventing ENaC degradation [36-38]. Consistent with this, SGK1$^{-/-}$ mice have a salt wasting phenotype, excreting more Na^+ than wild-type mice when on a low salt diet, leading to reduced blood pressure [39, 40]. SGK1$^{-/-}$ mice are also resistant to dexamethasone-induced increases in blood pressure [41] and display reduced glucocorticoid-induced intestinal glucose transport [42]. As SGK1 activity is reduced in the Protor-1$^{-/-}$Protor-2$^{-/-}$ double knockout mice, ENaC expression may also be lowered. However, we observed similar levels of ENaCα and ENaCγ subunits in membrane fractions derived from the kidney tissue of wild type and Protor-1$^{-/-}$ Protor-2$^{-/-}$ double knockout mice (Supplementary Fig 4), suggesting that Protor isoforms are not essential for normal regulation of basal ENaC expression in otherwise healthy unstressed animals. It would be interesting to test whether under conditions of salt challenge or in

hypertensive models, Protor isoforms play a more dominant role in the control of ENaC expression.

It will also be necessary to address the mechanism by which Protor regulates efficient activation of SGK1 in the kidney. Our studies suggest that loss of Protor isoforms does not impact on the ability of immunoprecipitated mTORC2 to phosphorylate SGK1 or Akt. This raises the possibility that Protor-1 may instead act as a scaffolding component to localise SGK1 to a particular location within the cell and/or to present SGK1 to mTORC2. In *S. cerevisiae* TORC2 there are two non-essential components termed Bit61 and AVO2 [2, 43], that have been implicated in binding two substrates of TORC2 (Slm1 and Slm2) [44, 45]. Although there is no obvious sequence similarity between Protor isoforms and Bit61 and AVO2, it would be interesting to investigate whether Protor isoforms performed a similar function. Thus far we have been unable to demonstrate a convincing co-immunoprecipitation of endogenous Protor-1 and SGK1 derived from kidney extracts. However, we cannot rule out the possibility that SGK1 and Protor-1 may interact with one another with low micromolar affinity. This would not be observed in co-immunoprecipitation studies, as the subunits would dissociate under the conditions and timeframe of such experiments.

In conclusion, our results establish that Protor-1 is required for SGK1 phosphorylation and signalling in the kidney. Further work is required to delineate the mechanism by which Protor-1 regulates efficient activation of SGK1 in the kidney and whether Protor isoforms are required for the activation of SGK1 and other SGK isoforms in other tissues and cell types. In addition, our data indicate that Protor-1 and Protor-2 play distinct roles and further work will be required to uncover the function of Protor-2. It is also possible that Protor isoforms play a key role in regulating mTORC2 function under conditions that we have not investigated. It is also possible that mTORC2 phosphorylates substrates other than Akt, SGK, and perhaps PKC isoforms, so in the future it will be important to investigate the role of Protor isoforms in controlling these, as yet uncharacterised, functions of mTORC2. The availability of Protor knockout mouse models and MEFs should prove useful for further studies to define the roles of Protor subunits in regulating mTORC2.

Acknowledgements.
We thank Gail Fraser for genotyping of the mice, the Sequencing Service (College of Life Sciences, University of Dundee, Scotland) for DNA sequencing and the protein production and antibody purification teams [Division of Signal Transduction Therapy (DSTT), University of Dundee] co-ordinated by Hilary McLauchlan and James Hastie. LRP is funded by an MRC UK Studentship and EMS is supported by an AstraZeneca supported BBSRC-CASE PhD Studentship. We thank the Medical Research Council, and the pharmaceutical companies supporting the Division of Signal Transduction Therapy Unit (AstraZeneca, Boehringer-Ingelheim, GlaxoSmithKline, Merck KgaA and Pfizer) for financial support.

Author Contributions.
LRP with the help of EMS performed most experiments, KS performed IGF1 injections and provided critical advice. LRP & SW performed the experiments shown in Supplementary Figure 1. LRP, EMS and DRA planned experiments, analysed the data and wrote the manuscript.

References

1 Guertin, D. A. and Sabatini, D. M. (2007) Defining the role of mTOR in cancer. Cancer cell. **12**, 9-22

2 Loewith, R., Jacinto, E., Wullschleger, S., Lorberg, A., Crespo, J. L., Bonenfant, D., Oppliger, W., Jenoe, P. and Hall, M. N. (2002) Two TOR complexes, only one of which is rapamycin sensitive, have distinct roles in cell growth control. Molecular cell. **10**, 457-468

3 Hara, K., Maruki, Y., Long, X., Yoshino, K., Oshiro, N., Hidayat, S., Tokunaga, C., Avruch, J. and Yonezawa, K. (2002) Raptor, a binding partner of target of rapamycin (TOR), mediates TOR action. Cell. **110**, 177-189

4 Kim, D. H., Sarbassov, D. D., Ali, S. M., King, J. E., Latek, R. R., Erdjument-Bromage, H., Tempst, P. and Sabatini, D. M. (2002) mTOR interacts with raptor to form a nutrient-sensitive complex that signals to the cell growth machinery. Cell. **110**, 163-175

5 Sancak, Y., Thoreen, C. C., Peterson, T. R., Lindquist, R. A., Kang, S. A., Spooner, E., Carr, S. A. and Sabatini, D. M. (2007) PRAS40 is an insulin-regulated inhibitor of the mTORC1 protein kinase. Molecular cell. **25**, 903-915

6 Huang, J. and Manning, B. D. (2008) The TSC1-TSC2 complex: a molecular switchboard controlling cell growth. The Biochemical journal. **412**, 179-190

7 Findlay, G. M., Yan, L., Procter, J., Mieulet, V. and Lamb, R. F. (2007) A MAP4 kinase related to Ste20 is a nutrient-sensitive regulator of mTOR signalling. The Biochemical journal. **403**, 13-20

8 Sancak, Y., Peterson, T. R., Shaul, Y. D., Lindquist, R. A., Thoreen, C. C., Bar-Peled, L. and Sabatini, D. M. (2008) The Rag GTPases bind raptor and mediate amino acid signaling to mTORC1. Science (New York, N.Y. **320**, 1496-1501

9 Kim, E., Goraksha-Hicks, P., Li, L., Neufeld, T. P. and Guan, K. L. (2008) Regulation of TORC1 by Rag GTPases in nutrient response. Nature cell biology. **10**, 935-945

10 Jacinto, E., Loewith, R., Schmidt, A., Lin, S., Ruegg, M. A., Hall, A. and Hall, M. N. (2004) Mammalian TOR complex 2 controls the actin cytoskeleton and is rapamycin insensitive. Nature cell biology. **6**, 1122-1128

11 Sarbassov, D. D., Ali, S. M., Kim, D. H., Guertin, D. A., Latek, R. R., Erdjument-Bromage, H., Tempst, P. and Sabatini, D. M. (2004) Rictor, a novel binding partner of mTOR, defines a rapamycin-insensitive and raptor-independent pathway that regulates the cytoskeleton. Curr Biol. **14**, 1296-1302

12 Yang, Q., Inoki, K., Ikenoue, T. and Guan, K. L. (2006) Identification of Sin1 as an essential TORC2 component required for complex formation and kinase activity. Genes & development. **20**, 2820-2832

13 Frias, M. A., Thoreen, C. C., Jaffe, J. D., Schroder, W., Sculley, T., Carr, S. A. and Sabatini, D. M. (2006) mSin1 is necessary for Akt/PKB phosphorylation, and its isoforms define three distinct mTORC2s. Curr Biol. **16**, 1865-1870

14 Jacinto, E., Facchinetti, V., Liu, D., Soto, N., Wei, S., Jung, S. Y., Huang, Q., Qin, J. and Su, B. (2006) SIN1/MIP1 maintains rictor-mTOR complex integrity and regulates Akt phosphorylation and substrate specificity. Cell. **127**, 125-137

15 Pearce, L. R., Huang, X., Boudeau, J., Pawlowski, R., Wullschleger, S., Deak, M., Ibrahim, A. F., Gourlay, R., Magnuson, M. A. and Alessi, D. R. (2007) Identification of

Protor as a novel Rictor-binding component of mTOR complex-2. The Biochemical journal. **405**, 513-522

16 Woo, S. Y., Kim, D. H., Jun, C. B., Kim, Y. M., Haar, E. V., Lee, S. I., Hegg, J. W., Bandhakavi, S., Griffin, T. J. and Kim, D. H. (2007) PRR5, a novel component of mTOR complex 2, regulates platelet-derived growth factor receptor beta expression and signaling. The Journal of biological chemistry. **282**, 25604-25612

17 Thedieck, K., Polak, P., Kim, M. L., Molle, K. D., Cohen, A., Jeno, P., Arrieumerlou, C. and Hall, M. N. (2007) PRAS40 and PRR5-like protein are new mTOR interactors that regulate apoptosis. PloS one. **2**, e1217

18 Pearce, L. R., Komander, D. and Alessi, D. R. (2010) The nuts and bolts of AGC protein kinases. Nature reviews. **11**, 9-22

19 Sarbassov, D. D., Guertin, D. A., Ali, S. M. and Sabatini, D. M. (2005) Phosphorylation and regulation of Akt/PKB by the rictor-mTOR complex. Science (New York, N.Y. **307**, 1098-1101

20 Garcia-Martinez, J. M. and Alessi, D. R. (2008) mTOR complex 2 (mTORC2) controls hydrophobic motif phosphorylation and activation of serum- and glucocorticoid-induced protein kinase 1 (SGK1). The Biochemical journal. **416**, 375-385

21 Ikenoue, T., Inoki, K., Yang, Q., Zhou, X. and Guan, K. L. (2008) Essential function of TORC2 in PKC and Akt turn motif phosphorylation, maturation and signalling. The EMBO journal. **27**, 1919-1931

22 Facchinetti, V., Ouyang, W., Wei, H., Soto, N., Lazorchak, A., Gould, C., Lowry, C., Newton, A. C., Mao, Y., Miao, R. Q., Sessa, W. C., Qin, J., Zhang, P., Su, B. and Jacinto, E. (2008) The mammalian target of rapamycin complex 2 controls folding and stability of Akt and protein kinase C. The EMBO journal. **27**, 1932-1943

23 Oh, W. J., Wu, C. C., Kim, S. J., Facchinetti, V., Julien, L. A., Finlan, M., Roux, P. P., Su, B. and Jacinto, E. (2010) mTORC2 can associate with ribosomes to promote cotranslational phosphorylation and stability of nascent Akt polypeptide. The EMBO journal. **29**, 3939-3951

24 Tessier, M. and Woodgett, J. R. (2006) Serum and glucocorticoid-regulated protein kinases: variations on a theme. Journal of cellular biochemistry. **98**, 1391-1407

25 Biondi, R. M., Kieloch, A., Currie, R. A., Deak, M. and Alessi, D. R. (2001) The PIF-binding pocket in PDK1 is essential for activation of S6K and SGK, but not PKB. The EMBO journal. **20**, 4380-4390

26 Collins, B. J., Deak, M., Arthur, J. S., Armit, L. J. and Alessi, D. R. (2003) In vivo role of the PIF-binding docking site of PDK1 defined by knock-in mutation. The EMBO journal. **22**, 4202-4211

27 Murray, J. T., Campbell, D. G., Morrice, N., Auld, G. C., Shpiro, N., Marquez, R., Peggie, M., Bain, J., Bloomberg, G. B., Grahammer, F., Lang, F., Wulff, P., Kuhl, D. and Cohen, P. (2004) Exploitation of KESTREL to identify NDRG family members as physiological substrates for SGK1 and GSK3. The Biochemical journal. **384**, 477-488

28 Betz, U. A., Vosshenrich, C. A., Rajewsky, K. and Muller, W. (1996) Bypass of lethality with mosaic mice generated by Cre-loxP-mediated recombination. Curr Biol. **6**, 1307-1316

29 Shioi, T., McMullen, J. R., Kang, P. M., Douglas, P. S., Obata, T., Franke, T. F., Cantley, L. C. and Izumo, S. (2002) Akt/protein kinase B promotes organ growth in transgenic mice. Molecular and cellular biology. **22**, 2799-2809

30 Rafiqi, F. H., Zuber, A. M., Glover, M., Richardson, C., Fleming, S., Jovanovic, S., Jovanovic, A., O'Shaughnessy, K. M. and Alessi, D. R. Role of the WNK-activated SPAK kinase in regulating blood pressure. EMBO Mol Med. **2**, 63-75

31 Wullschleger, S., Wasserman, D. H., Gray, A., Sakamoto, K. and Alessi, D. R. (2011) Role of TAPP1 and TAPP2 adaptor binding to PtdIns(3,4)P2 in regulating insulin sensitivity defined by knock-in analysis. The Biochemical journal. **434**, 265-274

32 Kumar, A., Harris, T. E., Keller, S. R., Choi, K. M., Magnuson, M. A. and Lawrence, J. C., Jr. (2008) Muscle-specific deletion of rictor impairs insulin-stimulated glucose transport and enhances Basal glycogen synthase activity. Molecular and cellular biology. **28**, 61-70

33 Kumar, A., Lawrence, J. C., Jr., Jung, D. Y., Ko, H. J., Keller, S. R., Kim, J. K., Magnuson, M. A. and Harris, T. E. (2010) Fat cell-specific ablation of rictor in mice impairs insulin-regulated fat cell and whole-body glucose and lipid metabolism. Diabetes. **59**, 1397-1406

34 Cybulski, N., Polak, P., Auwerx, J., Ruegg, M. A. and Hall, M. N. (2009) mTOR complex 2 in adipose tissue negatively controls whole-body growth. Proceedings of the National Academy of Sciences of the United States of America. **106**, 9902-9907

35 Loffing, J., Flores, S. Y. and Staub, O. (2006) Sgk kinases and their role in epithelial transport. Annual review of physiology. **68**, 461-490

36 Debonneville, C., Flores, S. Y., Kamynina, E., Plant, P. J., Tauxe, C., Thomas, M. A., Munster, C., Chraibi, A., Pratt, J. H., Horisberger, J. D., Pearce, D., Loffing, J. and Staub, O. (2001) Phosphorylation of Nedd4-2 by Sgk1 regulates epithelial Na(+) channel cell surface expression. The EMBO journal. **20**, 7052-7059

37 Snyder, P. M., Olson, D. R. and Thomas, B. C. (2002) Serum and glucocorticoid-regulated kinase modulates Nedd4-2-mediated inhibition of the epithelial Na+ channel. The Journal of biological chemistry. **277**, 5-8

38 Ichimura, T., Yamamura, H., Sasamoto, K., Tominaga, Y., Taoka, M., Kakiuchi, K., Shinkawa, T., Takahashi, N., Shimada, S. and Isobe, T. (2005) 14-3-3 proteins modulate the expression of epithelial Na+ channels by phosphorylation-dependent interaction with Nedd4-2 ubiquitin ligase. The Journal of biological chemistry. **280**, 13187-13194

39 Wulff, P., Vallon, V., Huang, D. Y., Volkl, H., Yu, F., Richter, K., Jansen, M., Schlunz, M., Klingel, K., Loffing, J., Kauselmann, G., Bosl, M. R., Lang, F. and Kuhl, D. (2002) Impaired renal Na(+) retention in the sgk1-knockout mouse. The Journal of clinical investigation. **110**, 1263-1268

40 Fejes-Toth, G., Frindt, G., Naray-Fejes-Toth, A. and Palmer, L. G. (2008) Epithelial Na+ channel activation and processing in mice lacking SGK1. American journal of physiology. **294**, F1298-1305

41 Boini, K. M., Nammi, S., Grahammer, F., Osswald, H., Kuhl, D. and Lang, F. (2008) Role of serum- and glucocorticoid-inducible kinase SGK1 in glucocorticoid regulation of renal electrolyte excretion and blood pressure. Kidney & blood pressure research. **31**, 280-289

42 Grahammer, F., Henke, G., Sandu, C., Rexhepaj, R., Hussain, A., Friedrich, B., Risler, T., Metzger, M., Just, L., Skutella, T., Wulff, P., Kuhl, D. and Lang, F. (2006) Intestinal function of gene-targeted mice lacking serum- and glucocorticoid-inducible kinase 1. Am J Physiol Gastrointest Liver Physiol. **290**, G1114-1123

43 Wullschleger, S., Loewith, R., Oppliger, W. and Hall, M. N. (2005) Molecular organization of target of rapamycin complex 2. The Journal of biological chemistry. **280**, 30697-30704

44 Audhya, A., Loewith, R., Parsons, A. B., Gao, L., Tabuchi, M., Zhou, H., Boone, C., Hall, M. N. and Emr, S. D. (2004) Genome-wide lethality screen identifies new PI4,5P2 effectors that regulate the actin cytoskeleton. The EMBO journal. **23**, 3747-3757

45 Fadri, M., Daquinag, A., Wang, S., Xue, T. and Kunz, J. (2005) The pleckstrin homology domain proteins Slm1 and Slm2 are required for actin cytoskeleton organization in yeast and bind phosphatidylinositol-4,5-bisphosphate and TORC2. Molecular biology of the cell. **16**, 1883-1900

Figure Legends

Table 1 Breeding strategy used to generate Protor-1$^{-/-}$, Protor-2$^{-/-}$ and Protor-1$^{-/-}$ Protor-2$^{-/-}$ knockout mice.
Single homozygous Protor-1$^{-/-}$, Protor-2$^{-/-}$ as well as Protor-1$^{-/-}$Protor-2$^{-/-}$ double knockout mice were bred using depicted strategy. The number and the percentage of each genotype are indicated followed by its expected Mendelian frequency. In the case of the Protor-1$^{-/-}$ Protor-2$^{-/-}$ double knockout mice, as wild-type littermate and double knock-in mice can only be obtained at a ratio of 1 in 16 in the same cross (Table 1), we interbred Protor-1$^{-/-}$ Protor-2$^{-/-}$ mice as well as Protor-1$^{+/+}$Protor-2$^{+/+}$ animals.

Figure 1 Generation of Protor-1$^{-/-}$ and Protor-2$^{-/-}$ knockout mice.
(**A**) Diagram depicting the Protor-1 targeting construct, the endogenous Protor-1 allele, the targeted allele obtained following homologous recombination, the Protor-1 conditional knockout allele with the neomycin cassette removed by Flp recombinase and the constitutive knockout allele obtained following Cre-mediated recombination. The light grey rectangles represent exons, black rectangles indicate the targeted exons and the dark grey and light grey triangles represent *loxP* and *FRT* sites, respectively. The positions of the 5' and 3' probes used for Southern blot analysis and the Protor-1 PCR primers (P1, P2 & P6) used for genotyping are indicated. The translation initiation sites for Protor-1α/β and Protor-1γ are within exons 2 and 4 respectively. (**B**) Genomic DNA purified from the targeted ES cells of the indicated genotypes was digested with either *BamHI* or *AseI* and subjected to Southern analysis with the corresponding DNA probes. In the case of the 5' probe, the wild type allele produces a 4.9kb fragment while the conditional knockout allele generates a 7kb fragment. The 3' probe detects a fragment of 25.5kb from the wild type allele and a 15.1kb fragment from the conditional knockout allele. (**C**) Genomic DNA was PCR amplified with Protor-1 primers P1, P2 and P6. The wild-type allele (detected using P1 and P2) generates a 290bp product while the knockout allele (detected using P1 and P6) generates a 559bp product. (**D**) Protor-1 was immunoprecipitated from each of the indicated mouse tissue lysates and HEK293 cell lysate and immunoblotting carried out using the same antibody. (**E**) Diagram depicting the Protor-2 targeting construct, the endogenous Protor-2 allele, the targeted allele obtained following homologous recombination, the Protor-2 conditional knockout allele and the constitutive knockout allele. The positions of the Protor-2 PCR primers (P1, P2 & P4) used for genotyping are indicated with arrows. The translation initiation site for Protor-2 is within exons 2. (**F**) Genomic DNA purified from the targeted ES cells of the indicated genotypes was digested with either *EcoRI* or *HindIII* and subjected to Southern analysis with the corresponding DNA probes. In the case of the 5' probe, the wild type allele produces a 6.8kb fragment while the conditional knockout allele generates a 9.8kb fragment. The 3' probe detects a fragment of 12kb from the wild type allele and a 10.6kb fragment from the conditional knockout allele. (**G**) Genomic DNA was PCR amplified with Protor-2 primers P1, P2 and P4. The wild-type allele (detected using P1 and P2) generates a 221bp product while the knockout allele (detected using P1 and P4) generates a 527bp product. (**H**) Protor-2 was immunoprecipitated from each of the indicated mouse tissue lysates and immunoblotting carried out using the same antibody.

Figure 2 NDRG1 phosphorylation is reduced in the kidney of Protor-1$^{-/-}$ knockout mice.
Tissue lysates from (**A**) Kidney, (**B**) Adipose, (**C**) Brain (**D**) Heart, (**E**) Liver (**F**) Lung (**G**) Muscle, (**H**) Spleen, or (**I**) Testis were generated from fed mice of the indicated genotype and subjected to immunoblotting with the indicated antibodies.

Figure 3 NDRG1 phosphorylation is reduced in the kidney of Protor-1$^{-/-}$ and Protor-1$^{-/-}$ Protor-2$^{-/-}$ knockout mice.
(**A**) Kidney lysates were generated from fed Protor-1$^{+/+}$, Protor-1$^{+/-}$ and Protor-1$^{-/-}$ mice and subjected to immunoblotting with the indicated antibodies. (**B**) As in (**A**) except lysates were from Protor-2$^{+/+}$, Protor-2$^{+/-}$ and Protor-2$^{-/-}$ mice. (**C**) As in (**A**) except lysates were from Protor-1$^{+/+}$Protor-2$^{+/+}$ and Protor-1$^{-/-}$Protor-2$^{-/-}$ mice.

Figure 4 Phosphorylation of SGK1 is reduced in the kidney of Protor-1$^{-/-}$ knockout mice.
(**A**) Protor-1$^{+/+}$Protor-2$^{+/+}$ and Protor-1$^{-/-}$Protor-2$^{+/+}$ mice were deprived of food for 3hrs and intravenously injected with 0.5μg/g body weight IGF1 or the equivalent amount of PBS as a negative control. After 5min, tissues were rapidly removed and frozen in liquid nitrogen. Kidney lysates were subjected to immunoblotting with the indicated antibodies and each lane represents a sample derived from a different mouse. (**B**) As in (**A**) except Protor-1$^{+/+}$Protor-2$^{+/+}$ and Protor-1$^{+/+}$Protor-2$^{-/-}$ were injected with IGF1. (**C**) As in (**A**) except Protor-1$^{+/+}$Protor-2$^{+/+}$ and Protor-1$^{-/-}$Protor-2$^{-/-}$ were injected with IGF1.

Figure 5 NDRG1 phosphorylation is normal in Protor deficient mouse embryonic fibroblasts (MEFs) .
The wild type and Protor-1$^{-/-}$Protor-2$^{-/-}$ deficient MEF cells were serum-starved overnight and stimulated with 50 ng/ml IGF1 for 30 min prior to lysis and immunoblot analysis with the indicated antibodies. Similar results were obtained in two separate experiments.

Figure 6 Protor-1 and Protor-2 are not required for mTORC2 complex formation *in vivo*.
(**A to C**) Sin1 was immunoprecipitated from kidney lysates obtained from mice of the indicated genotype and subjected to immunoblotting with the indicated antibodies. Similar results were obtained in two separate experiments.

Figure 7 Protor isoforms are not required for mTORC2 kinase activity *in vitro*.
(**A**) Immunoprecipitates were prepared using either pre-immune IgG (negative control) or Sin1 antibodies from fed wild type or Protor-1$^{-/-}$Protor-2$^{-/-}$ double knockout mouse kidney or liver lysates. Immunoprecipitates were incubated with GST-Akt1 in the presence of 0.1mM ATP and 10mM $MgCl_2$ for 30min at 30°C. Kinase reactions were analysed by immunoblotting with the indicated antibodies. (**B**) As in (**A**) except GST-ΔN-SGK1 [61-431] was used as the substrate in the mTORC2 kinase assay. (**C**) As in (**A**) except immunoprecipitates were generated from kidney or liver lysates from mice injected with IGF1 for 5min. (**D**) As in (**C**) except GST-ΔN-SGK1 [61-431] was used as the substrate in the mTORC2 kinase assay. (**E**) as in (**A**) except immunoprecipitates were prepared from wild type or Protor-1$^{-/-}$Protor-2$^{-/-}$ double knockout MEF cells. (**F**) as in (**E**) except GST-ΔN-SGK1 [61-431] was used as the substrate in the mTORC2 kinase assay. Similar results were obtained in two separate experiments.

Biochemical Journal Immediate Publication. Published on 18 Mar 2011 as manuscript BJ20102103

Cross	Genotype	Number	Expected Frequency
Protor-1$^{+/-}$ X Protor-1$^{+/-}$	Protor-1$^{+/+}$ Protor-1$^{+/-}$ Protor-1$^{-/-}$	163 (31.6%) 249 (48.3%) 104 (20.1%)	25% 50% 25%
Protor-2$^{+/-}$ X Protor-2$^{+/-}$	Protor-2$^{+/+}$ Protor-2$^{+/-}$ Protor-2$^{-/-}$	12 (15.2%) 42 (53.2%) 25 (31.6%)	25% 50% 25%
Protor-1$^{+/-}$ Protor-2$^{+/-}$ X Protor-1$^{+/-}$ Protor-2$^{+/-}$	Protor-1$^{+/+}$ Protor-2$^{+/+}$ Protor-1$^{-/-}$ Protor-2$^{-/-}$ Protor-1$^{+/-}$ Protor-2$^{+/-}$ Protor-1$^{+/-}$ Protor-2$^{+/+}$ Protor-1$^{+/+}$ Protor-2$^{+/-}$ Protor-1$^{-/-}$ Protor-2$^{+/+}$ Protor-1$^{+/+}$ Protor-2$^{-/-}$ Protor-1$^{-/-}$ Protor-2$^{+/-}$ Protor-1$^{+/-}$ Protor-2$^{-/-}$	8 (14.5%) 4 (7.3%) 7 (12.7%) 3 (5.5%) 14 (25.3%) 3 (5.5%) 3 (5.5%) 9 (16.4%) 4 (7.3%)	6.25% 6.25% 25% 12.5% 12.5% 6.25% 6.25% 12.5% 12.5%
Protor-1$^{+/+}$ Protor-2$^{+/+}$ X Protor-1$^{+/+}$ Protor-2$^{+/+}$	Protor-1$^{+/+}$ Protor-2$^{+/+}$	100%	100%
Protor-1$^{-/-}$ Protor-2$^{-/-}$ X Protor-1$^{-/-}$ Protor-2$^{-/-}$	Protor-1$^{-/-}$ Protor-2$^{-/-}$	100%	100%

TABLE 1

Biochemical Journal Immediate Publication. Published on 18 Mar 2011 as manuscript BJ20102103

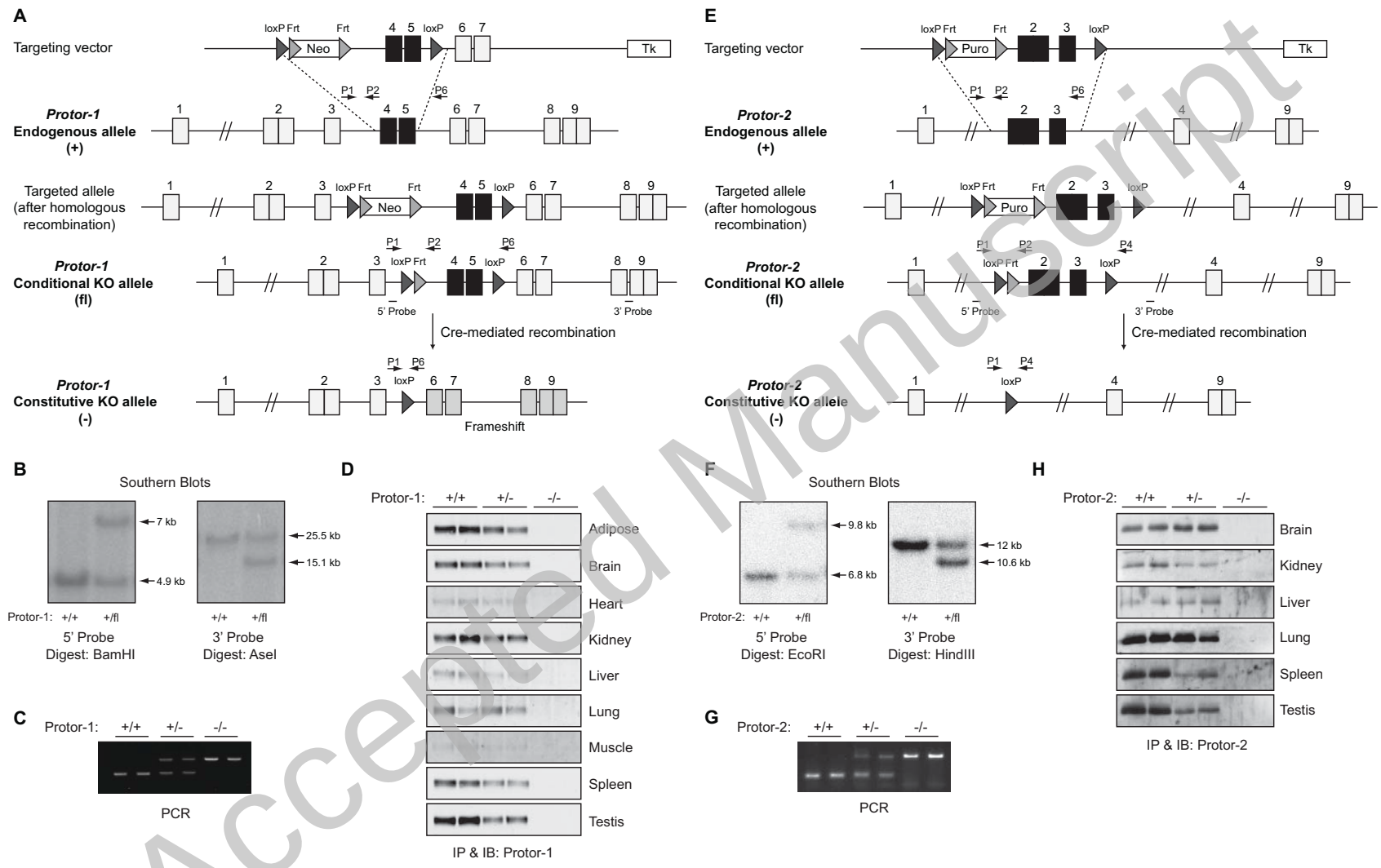

FIGURE 1

Biochemical Journal Immediate Publication. Published on 18 Mar 2011 as manuscript BJ20102103

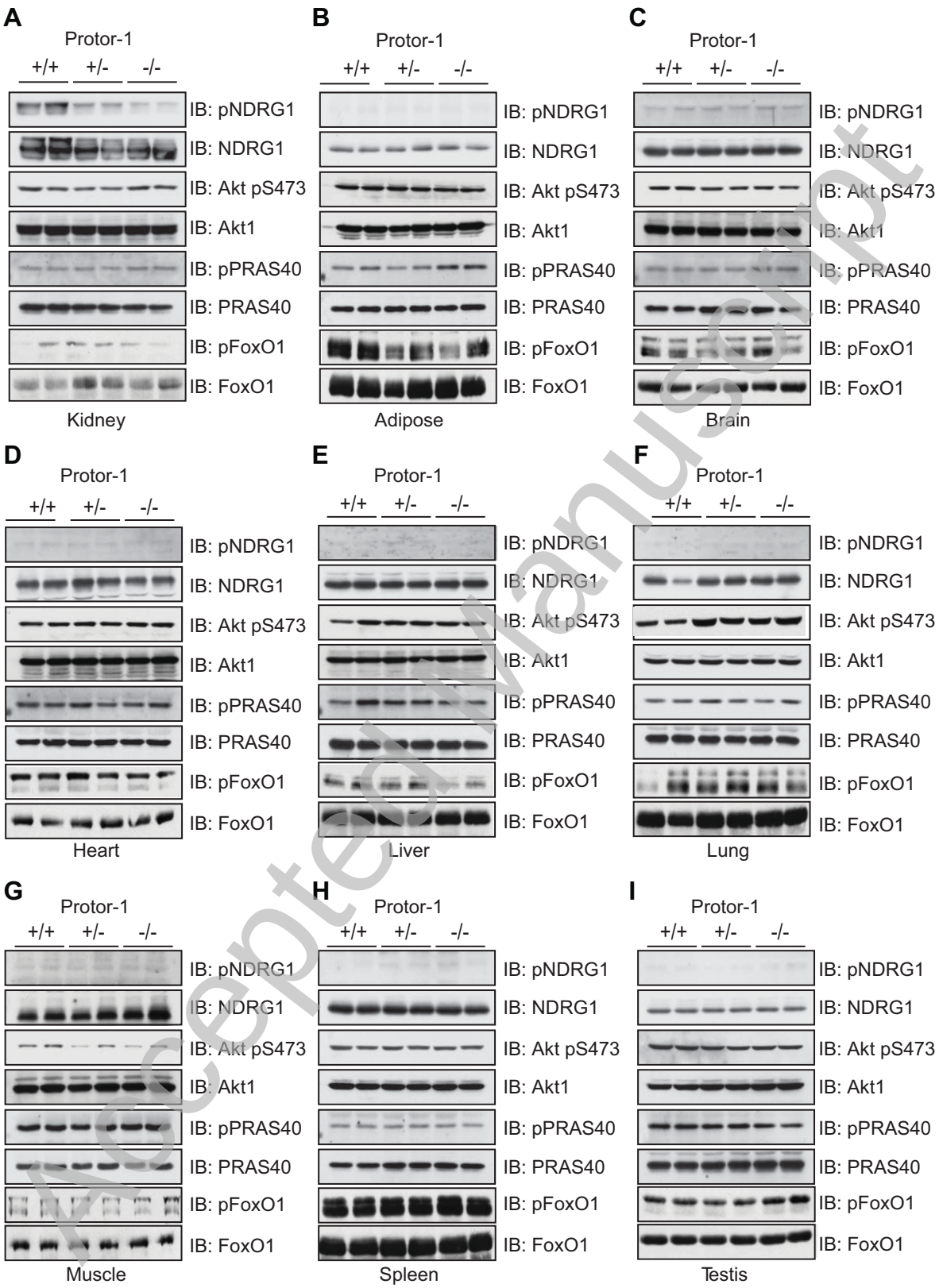

FIGURE 2

Biochemical Journal Immediate Publication. Published on 18 Mar 2011 as manuscript BJ20102103

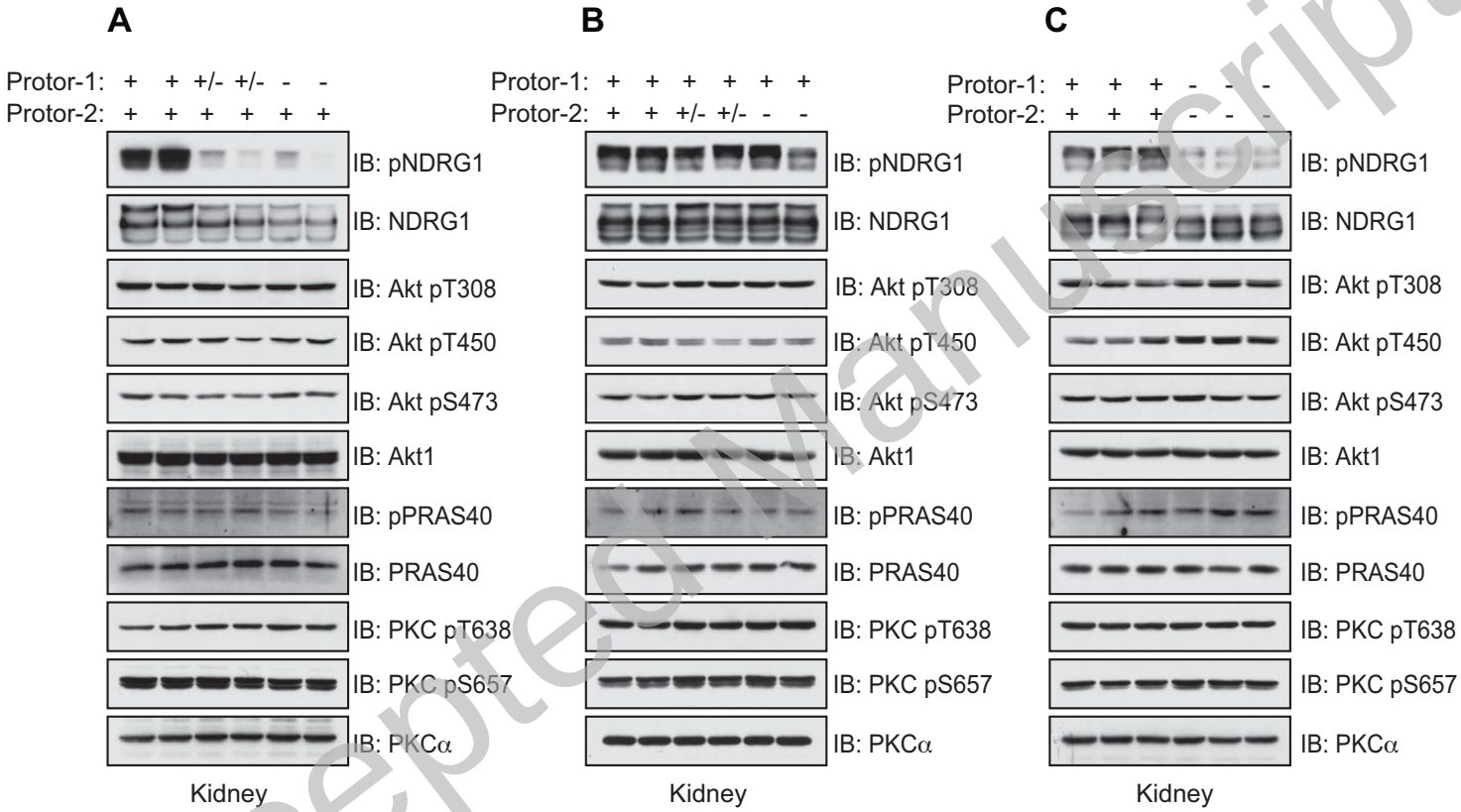

FIGURE 3

Biochemical Journal Immediate Publication. Published on 18 Mar 2011 as manuscript BJ20102103

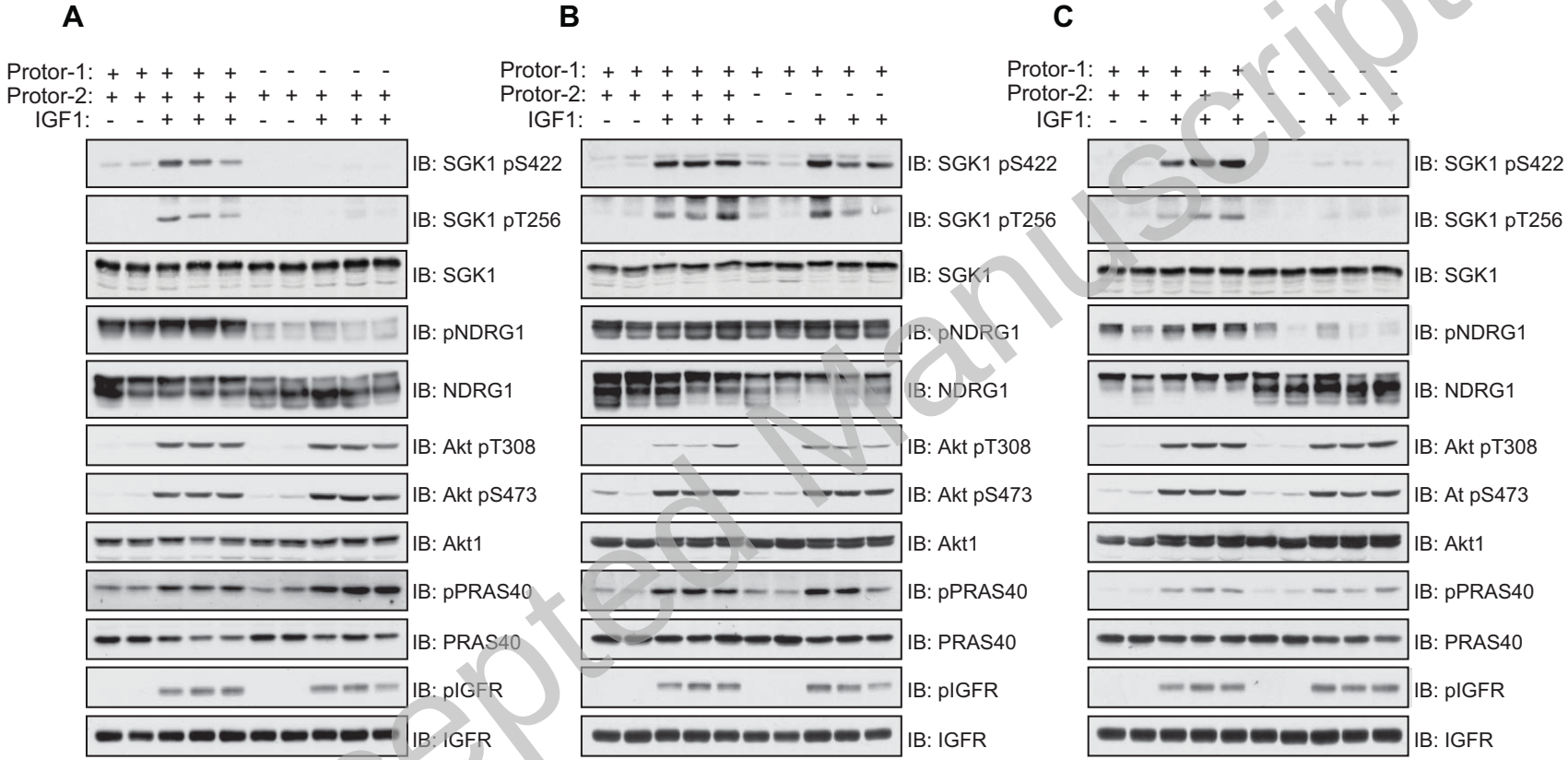

FIGURE 4

Biochemical Journal Immediate Publication. Published on 18 Mar 2011 as manuscript BJ20102103

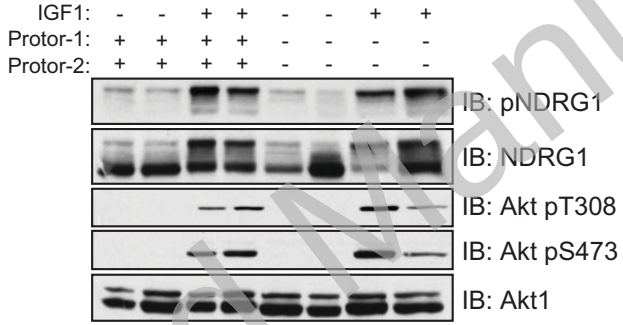

FIGURE 5

Biochemical Journal Immediate Publication. Published on 18 Mar 2011 as manuscript BJ20102103

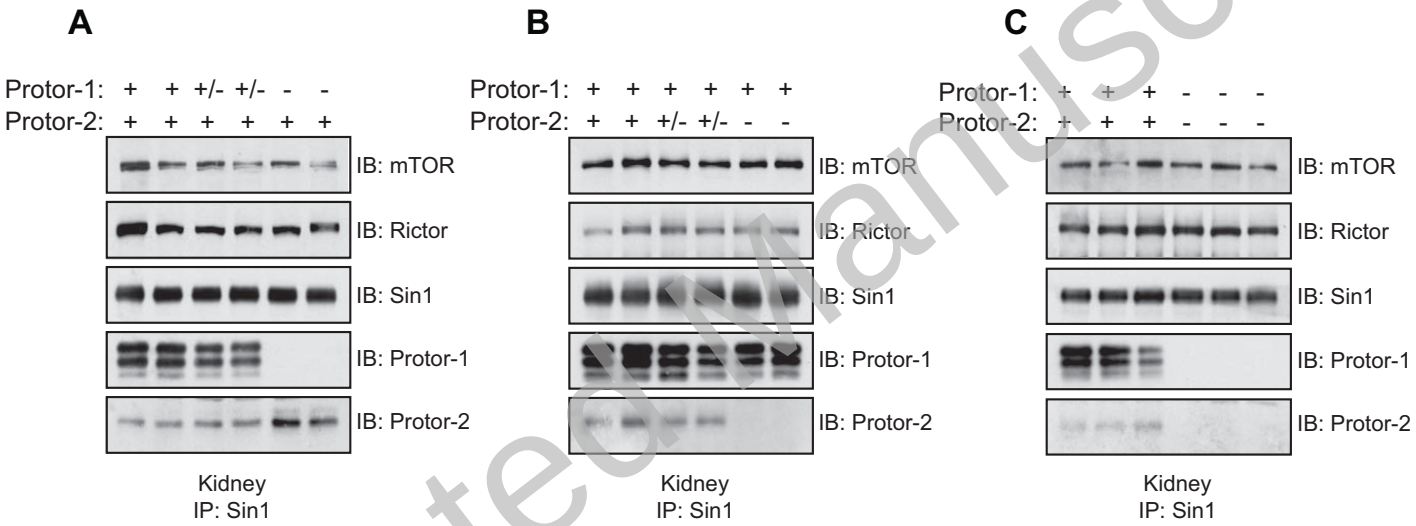

FIGURE 6

Biochemical Journal Immediate Publication. Published on 18 Mar 2011 as manuscript BJ20102103

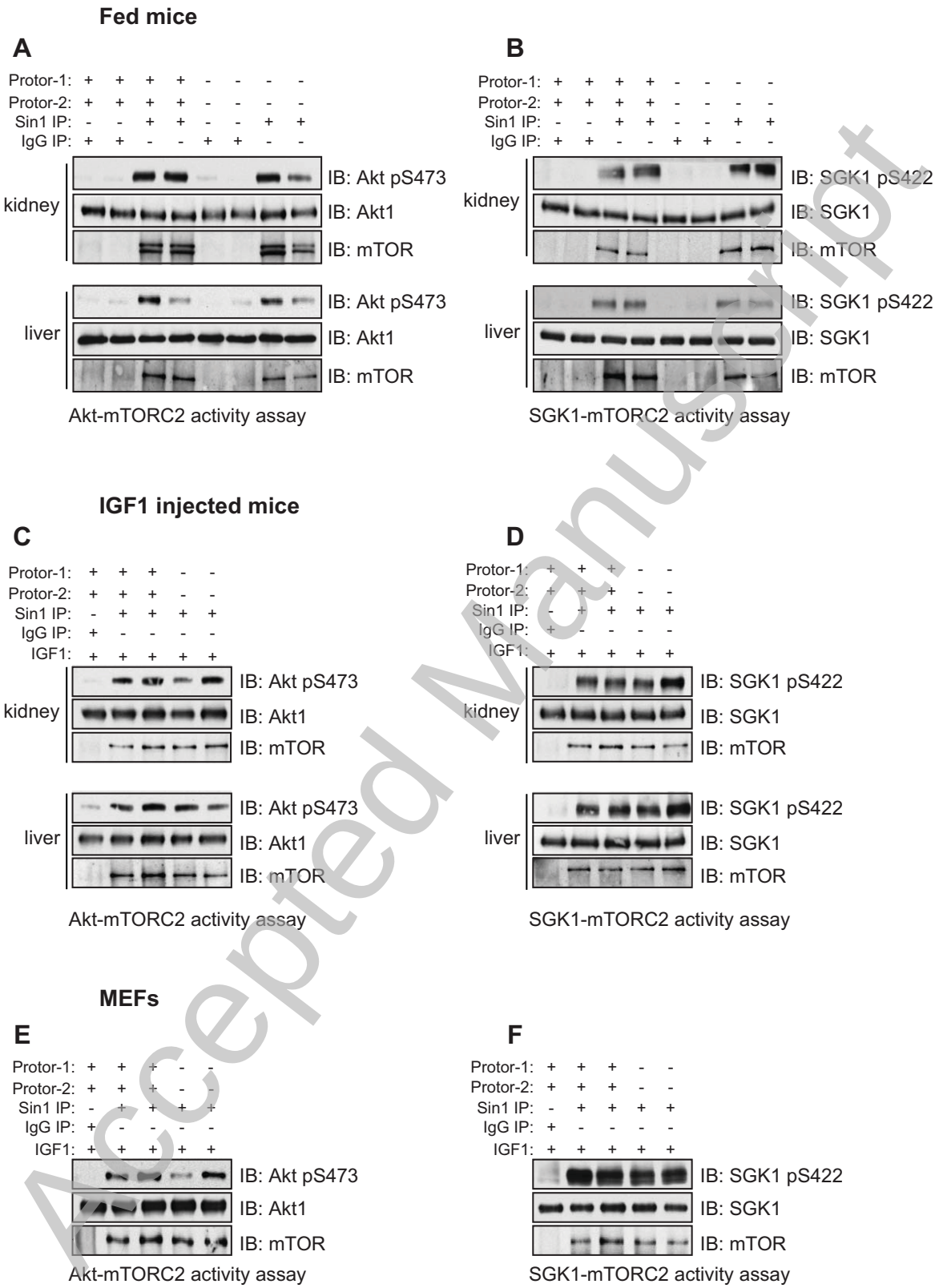

FIGURE 7